

Article

Parametric Investigation of a Ground Source CO₂ Heat Pump for Space Heating

Evangelos Bellos *  and Christos Tzivanidis 

Thermal Department, School of Mechanical Engineering, National Technical University of Athens, Zografou, Heron Polytechniou 9, 15780 Athens, Greece; ctzivan@central.ntua.gr

* Correspondence: bellose@central.ntua.gr

Abstract: The objective of the present study is the parametric investigation of a ground source heat pump for space heating purposes with boreholes. The working fluid in the heat pump is CO₂, and the geothermal field includes boreholes with vertical heat exchangers (U-tube). This study is conducted with a developed model in Engineering Equation Solver which is validated with data from the literature. Ten different parameters are investigated and more specifically five parameters about the heat pump cycle and five parameters for the geothermal unit. The heat pump's examined parameters are the high pressure, the heat exchanger effectiveness, the temperature level in the heater outlet, the flow rate of the geothermal fluid in the evaporator and the heat exchanger thermal transmittance in the evaporator. The other examined parameters about the geothermal unit are the ground mean temperature, the grout thermal conductivity, the inner diameter of the U-tube, the number of the boreholes and the length of every borehole. In the nominal design, it is found that the system's coefficient of performance is 4.175, the heating production is 10 kW, the electricity consumption is 2.625 kW, and the heat input from the geothermal field is 10.23 kW. The overall resistance of the borehole per length is 0.08211 mK/W, while there are 4 boreholes with borehole length at 50 m. The parametric analysis shows the influence of the ten examined parameters on the system's performance and on the geothermal system characteristics. This work can be used as a reference study for the design and the investigation of future geothermal-driven CO₂ heat pumps.

Keywords: geothermal energy; heat pump; space heating; CO₂; ground source heat pump



Citation: Bellos, E.; Tzivanidis, C. Parametric Investigation of a Ground Source CO₂ Heat Pump for Space Heating. *Energies* **2021**, *14*, 3563. <https://doi.org/10.3390/en14123563>

Academic Editors: Issa Chaer and Alessia Arteconi

Received: 3 May 2021
Accepted: 12 June 2021
Published: 15 June 2021

Publisher's Note: MDPI stays neutral with regard to jurisdictional claims in published maps and institutional affiliations.



Copyright: © 2021 by the authors. Licensee MDPI, Basel, Switzerland. This article is an open access article distributed under the terms and conditions of the Creative Commons Attribution (CC BY) license (<https://creativecommons.org/licenses/by/4.0/>).

1. Introduction

The building sector is responsible for a great amount of CO₂ emissions because this sector covers a great percentage of the worldwide energy consumption which is around 40% [1]. This fact creates the need for determining efficient ways in order to reduce the carbon footprint of the building sector in the environment. The use of renewable energy sources like solar energy, geothermal energy and biomass is an interesting idea in this direction [2]. Renewable energy sources can be used for direct electricity production (e.g., with photovoltaics) [3] or for heat production (solar thermal collectors or geothermal energy) [4] or to feed sorption machines for cooling [5].

Geothermal energy is a promising energy source that can be used for various applications like space-heating, electricity production and space-cooling systems for achieving higher efficiency [6]. Therefore, the geothermal-based units are sustainable ways for enhancing the energy performance of future systems, mainly in the building sector and in the domain of electricity. The high availability of geothermal energy, especially for applications like space-heating, makes the use of geothermal energy a very attractive choice for achieving sustainability [7].

In the literature, there are many studies in the field of geothermal-driven heat pumps. There are different designs with horizontal heat exchangers, vertical heat exchangers (borehole) and underground thermal storage systems [8]. In 2012, Karytsas [9] conducted

a detailed review of different geothermal-assisted heat pumps and concluded that they are more efficient than the conventional systems about 50% to 80%. In 2013, Michopoulos et al. [10] performed a detailed work about the performance of a geothermal-driven heat pump with vertical boreholes for the heating and cooling period in Northern Greece. They found that the seasonal performance of the system to be around 5 in the heating period and around 4 in the cooling period. Zhang et al. [11] examined the idea of using an absorption heat pump driven by geothermal energy for heating purposes. They concluded that the examined idea enhances the energy efficiency by 54% and leads to 30% lower yearly operating costs.

Another interesting part of the literature includes studies about the combination of solar and geothermal energies for heating purposes. Emmi et al. [12] compared the use of a geothermal energy system with a solar-geothermal system for feeding a heat pump. They used solar flat plate collectors, and they found that the system without solar field presents about 10% lower efficiency than the system with solar and geothermal energy sources. Sakellariou et al. [13] studied a hybrid system with thermal photovoltaic collectors and a ground storage system for feeding a heat pump for heating purposes. They concluded that their design is about 22% more efficient than the base scenario.

In the last years, there have been regulations about the use of natural refrigerants and environmentally friendly refrigerants in heat pumps and in the building sector [14]. The most usual natural refrigerants are CO₂ (R744), R600, R600a, R290 and NH₃ [15]. In this direction, there are some literature studies that examine the use of CO₂ refrigerants in the heat pump. CO₂ is a non-toxic, non-flammable fluid, with zero ozone depletion potential and an extremely low global working potential equal to 1 [16]. Kim et al. [17] investigated a ground source heat pump with CO₂ which is applied for heating purposes. The produced heating from the heat pump condenser is stored in a storage tank and also solar collectors are used for assisting the stored heating in the tank. The heat pump coefficient of performance (COP) was calculated at 2.8. Eslami-Nejad et al. [18] examined a direct expansion heat pump driven by geothermal boreholes. They found that the system COP is around 3.

Moreover, it is important to note some interesting studies in the literature about the investigation of the geothermal field evaluation. Molina-Giraldo et al. [19] have investigated in detail the thermal dispersion on temperature plumes in geothermal configurations. They used analytical methods, and they calculated the length of the temperature plume. Piga et al. [20] performed a comparative study between the simplified and the rigorous methods in the systems with ground source heat pumps. They concluded that the simplified models can predict properly the plume length, while the proper calculation of the plume width needs the use of rigorous methods. Antelmi et al. [21] conducted a study about the thermal perturbation in groundwater for a system with boreholes. They found that higher groundwater velocity increases the heat transfer rates. Moreover, Antelmi et al. [22] performed a work about a reversible CO₂ heat pump for application in the building sector, and they found 22% higher performance of their system compared to a conventional one.

The objective of the present work is the parametric investigation of a geothermal-based heat pump for heating purposes with CO₂ as the working fluid. The novelty of this work is based on the use of a transcritical CO₂ heat pump coupled with a geothermal field which is something that is not usual in the literature. The importance of this work is based on the detailed parametric investigation of the examined system by performing parametric studies with ten different parameters. Therefore, the system was studied in various design and operating conditions, and the most effective designs for achieving maximum performance are found in this work. The analysis was conducted with a developed mathematical model in Engineering Equation Solver [23]. The developed model is validated by utilizing literature data about the heat pump and about the geothermal field. The results of this work can be used for designing the future geothermal-based heat pump and for their proper evaluation.

2. Materials and Methods

2.1. The Examined Geothermal-Based Unit

Figure 1 shows the investigated geothermal-based heat pump with CO₂ as the working fluid. The heat pump is a one-stage system with an internal heat exchanger which operates in transcritical mode. The reason for operating in the transcritical mode is the low critical temperature of the CO₂ at 31.1 °C, and therefore, there is a need to operate at a higher temperature level in order to produce space-heating. The heat pump is fed by heat input from the geothermal field and consumes electricity in order to produce heating at the proper temperature level. In this work, it is supposed that there is a proper system for extracting the heating from the “heater”. The temperature in the heater outlet is a parameter that is examined parametrically in this work. Furthermore, the high pressure of the cycle and the heat exchanger effectiveness are studied parametrically. The temperature level in the gas cooler outlet is selected at $T_5 = 25\text{ °C}$ which is an assumption of this work. However, the variation of this parameter has not so important an influence on the results. Moreover, it has to be said that the heating production is selected at $Q_{\text{heat}} = 10\text{ kW}$ in all the examined scenarios.

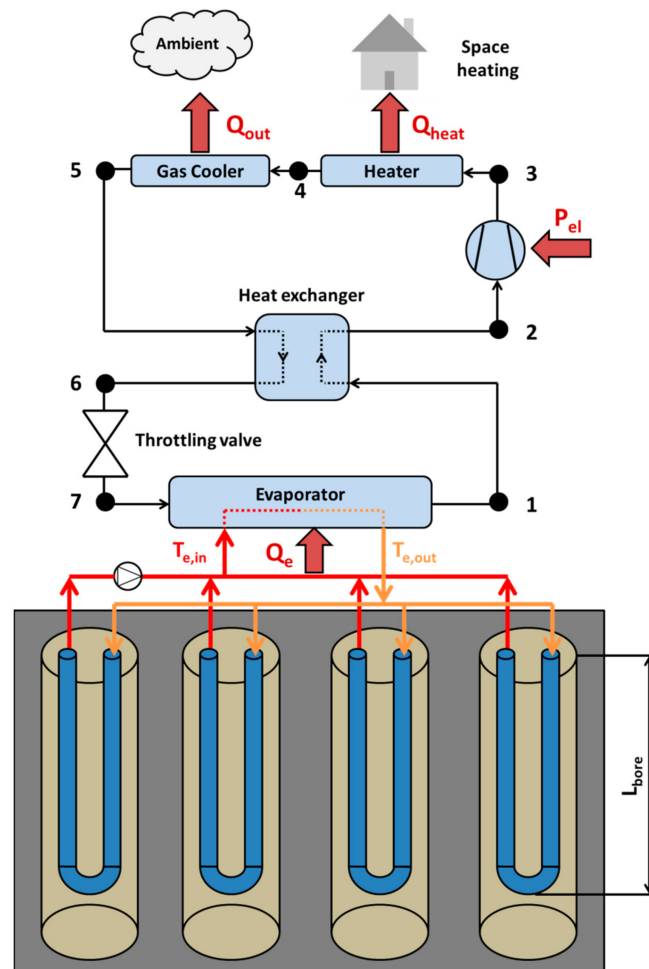


Figure 1. The investigated geothermal-based heat pump.

The geothermal field consists of boreholes that feed the evaporator with heat. The number of the boreholes and the borehole length are important parameters that are examined parametrically in the present study. Moreover, the mean temperature of the ground and the thermal conductivity of the grout are examined parametrically in order to study the system in different conditions. The analysis takes into consideration important parameters such as the diameter of the inner tube in the borehole (U-tube), the total thermal trans-

mittance in the evaporator $(UA)_e$ and the volumetric geothermal fluid flow rate. Table 1 includes the parameters that were studied parametrically, their default values and the examined range of every parameter. It is important to state that many data have been taken by ASHRAE guidelines [24], while the default means temperature regards the mean yearly temperature of Athens (Greece) [25]. In this work, it is assumed that there is a proper distance between the boreholes in order to avoid the thermal interaction between them.

Table 1. Parameters of the parametric analysis.

Parameter	Symbol	Default Value	Range
High pressure	P_{high}	85 bar	[80 to 100] bar
Heat exchanger effectiveness	η_{HEX}	90%	[0 to 100]%
Temperature in the heater outlet	T_4	35 °C	[32 to 38] °C
Volumetric flow rate in the evaporator	V_f	2 L/s	[1 to 5] L/s
Thermal transmittance in the evaporator	$(UA)_e$	3 kW/K	[1 to 5] kW/K
Ground temperature	T_g	18.6 °C	[10 to 22] °C
Thermal conductivity of the grout	k_{grt}	2.1 W/mK	[0.5 to 4.0] W/mK
Inner diameter of the U-tube	d_{in}	0.025 m	[0.015 to 0.040] m
Number of boreholes	N	4	[1 to 10]
Bore length	L_{bore}	50 m	[20 to 100] m

At this point, it is useful to explain the selected values in the parametric study which are included in Table 1. The examined range about the selected ground temperature is 10 °C to 22 °C which is a representative range for Mediterranean countries like Greece and Italy. For example, in Athens (Greece), the mean soil temperature can be around 18.6 °C [25]. The high pressure is selected to be between 80 bar in order to be over the critical pressure and up to 100 bar in order to avoid the extremely high pressure in a building heat pump. The borehole length has been examined from 20 m to 100 m which are acceptable values for a vertical geothermal field, and these values can supply the proper heat input in the system for the present design.

It has also to be said that the present work is conducted by a developed mathematical model in Engineering Equation Solver [23]. This software is a mathematical tool that solves iteratively non-linear equations, and also, it includes libraries for determining the thermodynamic properties and the thermal properties of the working fluids. In this work, the developed mathematical modeling includes the equations that are presented in Section 2.2 which are solved all together as a non-linear system by the software.

2.2. Mathematical Formulation

The examined unit is studied by developing a proper mathematical model in Engineering Equation Solver [23]. The equations of the present section are used in the created program for the proper simulation of the examined system.

2.2.1. Heat Pump Modeling

The heat input in the evaporator (Q_e) is calculated as below:

$$Q_e = \dot{m}_r \cdot (h_1 - h_7) \quad (1)$$

The electricity consumption in the compressor (P_{el}) is calculated as below:

$$P_{el} = \dot{m}_r \cdot (h_3 - h_2) \quad (2)$$

At this point, it has to be said that Equation (2) calculates the electricity because, in this work, the global efficiency is used for the modeling which is given in Equation (8) [26].

The heat capacity in the heater (Q_{heat}) is calculated as below:

$$Q_{heat} = \dot{m}_r \cdot (h_3 - h_4) \quad (3)$$

It has to be said that there is a need to design a proper heater in order to absorb efficiently the heat from the CO₂ with safety. The use of an increased flow rate in the water circuit will make possible the heating production at the desired levels.

The heat capacity in the ambient from the gas cooler (Q_{out}) is given as:

$$Q_{out} = \dot{m}_r \cdot (h_4 - h_5) \quad (4)$$

The use of the gas cooler aims to make a proper reduction in the CO₂ temperature in order to enhance the system efficiency.

The coefficient of performance in the heat pump (COP) is defined as follows:

$$COP = \frac{Q_{heat}}{P_{el}} \quad (5)$$

The energy balance in the heat exchanger can be written as below:

$$(h_2 - h_1) = (h_5 - h_6) \quad (6)$$

The heat exchanger effectiveness (η_{HEX}) is defined as follows:

$$\eta_{HEX} = \frac{T_2 - T_1}{T_5 - T_1} \quad (7)$$

The global efficiency of the compressor, which includes the isentropic and the mechanical efficiency is calculated according to the following formula [26]:

$$\eta_{comp} = 0.5168 + 0.0664 \cdot \pi_c - 0.0137 \cdot \pi_c^2 + 6 \cdot 10^{-14} \cdot \pi_c^3 - 4 \cdot 10^{-15} \cdot \pi_c^4 \quad (8)$$

where the parameter (π_c) is the pressure ratio in the compressor.

The expansion in the throttling valve is a process where there is no heat loss; thus, it can be said:

$$h_6 = h_7 \quad (9)$$

2.2.2. Heat Transfer in the Evaporator

The heat transfer rate at the evaporator between the CO₂ in temperature (T_e) and the geothermal fluid, which has inlet temperature ($T_{e,in}$) and outlet temperature ($T_{e,out}$) from the evaporator, can be modeled as below:

$$Q_{evap} = \dot{m}_f \cdot c_{p,f} \cdot (T_{e,in} - T_{e,out}) \quad (10)$$

$$Q_{evap} = (UA)_e \cdot \Delta T_{lm} \quad (11)$$

where the mean logarithmic temperature difference is written as below:

$$\Delta T_{lm} = \frac{T_{e,in} - T_{e,out}}{\ln \left[\frac{T_{e,in} - T_e}{T_{e,out} - T_e} \right]} \quad (12)$$

Moreover, it is useful to state that the mass flow rate of the total geothermal fluid (\dot{m}_f) which flows in the evaporator is connected with the volumetric flow rate (V_f) as follows:

$$\dot{m}_f = \rho_f \cdot V_f \quad (13)$$

2.2.3. Geothermal Field Modeling

The heat transfer is modeled by using the proper thermal resistances according to the ASHRAE methodology [24]. Below, the main steps of this methodology are described.

In the geothermal field, there is a different number of boreholes in every examined scenario which is symbolized as (N). Therefore, the total mass flow rate (\dot{m}_f) which passes

through the evaporator to be separated into (N) equal parts. Therefore, the mass flow rate of the fluid in every geothermal borehole ($\dot{m}_{f,0}$) is calculated as below:

$$\dot{m}_{f,0} = \frac{\dot{m}_f}{N} \quad (14)$$

The fluid that leaves the evaporator has a temperature ($T_{e,out}$), and it enters the geothermal borehole where it is heated up to the temperature ($T_{e,in}$) for feeding the evaporator. The mean fluid temperature in the geothermal field ($T_{f,m}$) is estimated as [24]:

$$T_{f,m} = \frac{T_{e,in} + T_{e,out}}{2} \quad (15)$$

In every examined case, the thickness of the U-tube is 3.5 mm, so it can be said about the inner diameter (d_{in}) and outer diameter (d_{out}) [24]:

$$d_{out} = d_{in} - 0.07 \text{ [m]} \quad (16)$$

The heat transfer rate from the ground to the geothermal fluid is equal to the heat input in the evaporator. Therefore, it can be said [24]:

$$Q_e = N \cdot \frac{L_{bore} \cdot (T_g - T_{f,m})}{R_{ov}} \quad (17)$$

The overall thermal resistance per length (R_{ov}) is calculated as a summary of other thermal resistances according to the ASHRAE methodology [24]. Therefore, the overall resistance (R_{ov}) is the sum of the heat exchanger thermal resistance (R_p) and the grout thermal resistance (R_{grt}). More specifically, the heat exchanger thermal resistance (R_p) includes the thermal resistance of the U-tube and the film thermal resistance of the fluid. This modeling assumes that there are not many fluctuations during the operation, because the heating load demand is assumed to be constant, and the system is approximately in steady-state conditions. Below, the definitions of the thermal resistances are given in detail:

$$R_{ov} = R_p + R_{grt} \quad (18)$$

The thermal resistance of the heat exchanger (U-tube) is normalized to the borehole length. For a single (U-tube), it can be said:

$$R_p = \frac{R_{film} + R_{tube}}{2} \quad (19)$$

The thermal resistance between the geothermal fluid and the tube (R_{film}) is defined as follows:

$$R_{film} = \frac{1}{\pi \cdot d_{in} \cdot h_f} \quad (20)$$

The thermal resistance of the tube (R_{tube}) is defined as follows:

$$R_{tube} = \frac{\ln \left[\frac{d_{out}}{d_{in}} \right]}{2 \cdot \pi \cdot k_{tube}} \quad (21)$$

The grout thermal resistance (R_{grt}) is the thermal resistance of the material in the local region of the borehole. The diameter of the borehole is symbolized with (d_p), and it can be said [23] that

$$R_{grt} = \left(k_{grt} \cdot b_0 \cdot \left[\frac{d_p}{d_{out}} \right]^{b1} \right)^{-1} \quad (22)$$

where the coefficients of the aforementioned formula are selected as ($b_0 = 21.91$) and ($b_1 = -0.3797$) for a borehole with the U-tube near the grout border region [24].

At this point, it is useful to state that the fluid heat transfer coefficient (h_f) is calculated by using the Nusselt Number. The definition of the Nusselt number (Nu) for a circular tube is given as

$$\text{Nu} = \frac{h_f \cdot d_{\text{in}}}{k_f} \quad (23)$$

The Reynolds number (Re) is a characteristic parameter of the flow, and it can be written as below for a circular tube:

$$\text{Re} = \frac{4 \cdot m_{f,0}}{\pi \cdot d_{\text{in}} \cdot \mu_f} \quad (24)$$

The Nusselt number for turbulent flow can be calculated according to the Colburn equation [27]. In this work, the Reynolds number has values in the turbulent flow regime, and therefore, this formula is a proper one.

$$\text{Nu} = 0.023 \cdot \text{Re}^{0.8} \cdot \text{Pr}_f^{1/3} \quad (25)$$

The Prandtl number (Pr_f) of the fluid is defined as below:

$$\text{Pr}_f = \frac{\mu_f \cdot c_{p,f}}{k_f} \quad (26)$$

2.3. Validation of the Developed Model

The validation of the CO₂ heat pump is performed by comparing the developed model with literature results from the Reference [26]. Table 2 includes the comparative results about the COP for different operating conditions. More specifically, different combinations of evaporator temperature and high pressure have been examined, and the results show that the mean deviation is about 3.22% which is an acceptable value. The temperature after the heater has been selected to be $T_4 = 34$ °C for conducting a proper comparative study.

Table 2. Validation evidence about the heat pump cycle with Reference [26].

T_e (°C)	P_{high} (bar)	COP Experimental	COP Simulation	COP Deviation
0.3	82.6	3.36	3.272	2.62%
−0.4	91.4	3.36	3.144	6.43%
−0.1	100.6	3.14	3.016	3.95%
0.8	112.6	2.86	2.885	0.87%
−0.6	100.0	3.04	2.996	1.45%
0.4	90.2	3.34	3.218	3.65%
1.0	98.9	3.06	3.114	1.76%
1.2	108.4	3.02	2.971	1.62%
−0.1	85.4	3.47	3.241	6.60%

The next part of the validation procedure regards the geothermal system. The overall resistance per length of the borehole is calculated in the default scenario at $R_{\text{ov}} = 0.08211$ mK/W, while Reference [23] gives the value of 0.08 mK/W for the same conditions. Therefore, there is a deviation of 2.63% which is a relatively low value. Therefore, the present model gives a correct calculation about the geothermal system resistance.

3. Results and Discussion

3.1. Investigation of the Default Scenario

The first part of the present study is the parametric investigation of the developed model. The default values of the examined parameters are used in order to provide

a detailed description of the examined unit in this case. The default values are given in Table 1. The results of the simulation for this scenario are included in Table 3. It is obvious that the COP is 4.175, the electricity consumption is 2.395 kW, the heat production 10 kW, the heat input in the evaporator from the geothermal field is 10.23 kW, and the heat rejection to the ambient from the gas cooler is 2.625 kW. Moreover, it has to be said that the compressor efficiency is 59.27%, the low-pressure level of the cycle is 46.1 bar, and the evaporator temperature is 10.96 °C. In the geothermal field, the fluid enters the U-tube at 13.79 °C and leaves the geothermal field for feeding the evaporator at 15.01 °C. The heat transfer coefficient from the fluid to the tube is 3185 W/m²K, and the overall resistance per length in the geothermal field is found at 0.08211 mK/W. At this point, it is worthy to comment that the found value of the COP at 4.175 is a promising one because it is higher than other results in the literature. For example, the COP of CO₂ transcritical heat pump driven by solar and geothermal energies has been found to be 2.81 [17], while a direct expansion CO₂ transcritical heat pump driven by geothermal energy presents a COP of 3.17 [18].

Table 3. Data for the default design scenario.

Parameter	Symbol	Value
Heating production	Q_{heat}	10 kW
Electricity Consumption	P_{el}	2.395 kW
Heat input in the evaporator	Q_{e}	10.23 kW
Heat rejection from the gas cooler	Q_{out}	2.625 kW
Coefficient of performance	COP	4.175
Compressor efficiency	η_{com}	59.27%
Overall Resistance	R_{ov}	0.08211 mK/W
Fluid heat transfer coefficient	h_{f}	3185 W/m ² K
Evaporator temperature	T_{e}	10.96 °C
Fluid inlet temperature in the evaporator	$T_{\text{e,in}}$	15.01 °C
Fluid outlet temperature in the evaporator	$T_{\text{e,out}}$	13.79 °C
Low pressure	P_{low}	46.1 bar

The next step in the preliminary analysis of the default scenario is the thermodynamic investigation of the CO₂ heat pump cycle. Table 4 includes the thermodynamic state points of the examined cycle (state points 1 to 7). More specifically, the temperature, the pressure, the specific enthalpy and the specific entropy of the state points are given in this table. Furthermore, the thermodynamic depictions of this cycle are provided in order to present it properly. Figure 2 shows the temperature–specific entropy depiction, while Figure 3 exhibits the pressure–specific enthalpy depiction. It is obvious that the examined cycle is a transcritical cycle with a low-pressure level at 46.1 bar and a high-pressure level at 85 bar. In the compressor inlet, there is superheating due to the existence of the heat exchanger, something important in order to achieve a subcooling after the gas cooler and also to control properly the mass flow rate of the refrigerant in a real application.

Table 4. Thermodynamic properties of the heat pump cycle in the basic operating scenario.

State Points	Temperature (T)	Pressure (p)	Specific Enthalpy (s)	Specific Entropy (h)
	[°C]	[bar]	[kJ/kg]	[kJ/kg K]
1	10.96	46.1	−84.95	−0.961
2	23.60	46.1	−59.09	−0.872
3	83.01	85.0	−15.36	−0.821
4	35.00	85.0	−197.90	−1.388
5	25.00	85.0	−245.80	−1.546
6	16.16	85.0	−271.70	−1.634
7	10.96	46.1	−271.70	−1.618

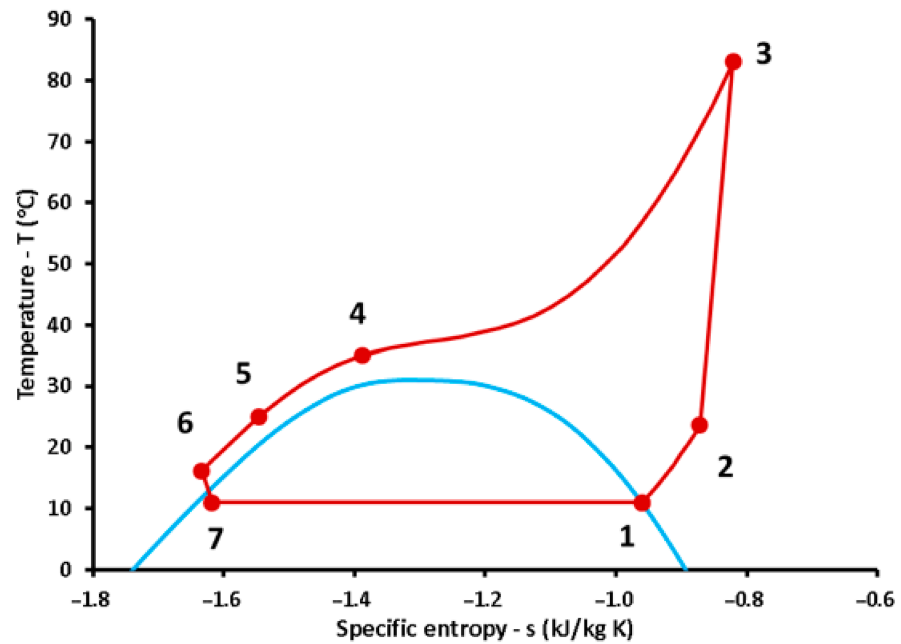


Figure 2. Pressure–specific entropy depiction of the heat pump cycle for the default scenario.

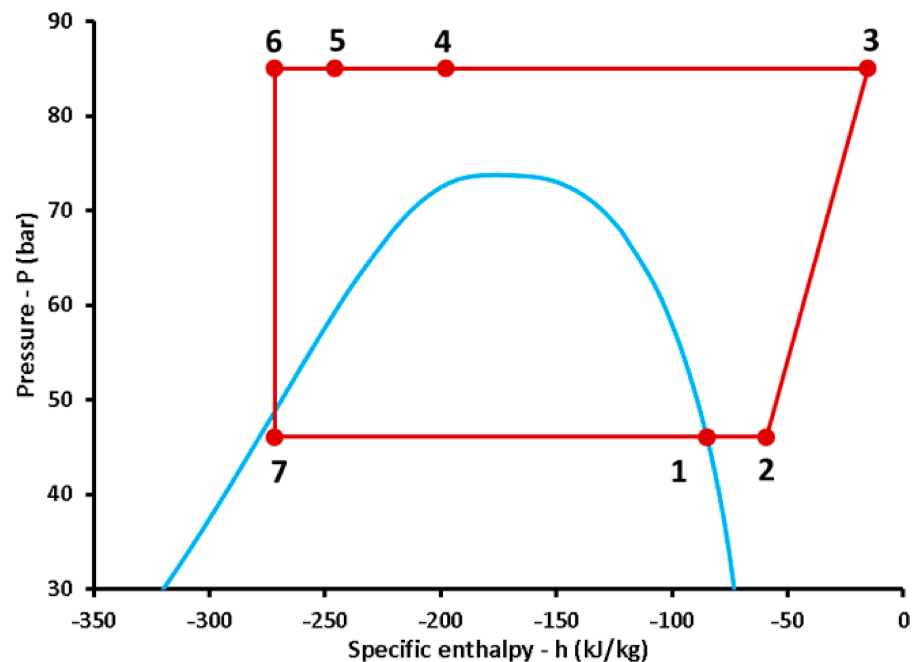


Figure 3. Pressure–specific enthalpy depiction of the heat pump cycle for the default scenario.

3.2. Parametric Investigation

The next part of the present work is the parametric investigation of the examined system. In every case, only one parameter changes while all the other parameters keep their default values according to Table 1. Moreover, the range of all the examined parameters is given in Table 1. These parameters are selected as critical design and operating parameters, and their investigation presents high interest to the readers. In every case, the COP, the electricity consumption, the heat input in the evaporator, the overall resistance of the geothermal field, the evaporator temperature, the fluid temperature in the evaporator inlet

and the fluid temperature in the evaporator outlet are presented as the most representative results for evaluating the present unit.

3.2.1. Heat Pump Parameters

The first part of the parametric investigation regards the investigation of parameters that are associated with the heat pump. More specifically, the studied parameters are the high pressure, the heat exchanger effectiveness, the temperature level in the heater outlet, the flow rate of the geothermal fluid in the evaporator and the heat exchanger thermal transmittance in the evaporator. These are important parameters that have to be studied in detail in order to investigate different design parameters that can influence the unit performance.

The first examined parameter is the high-pressure level of the heat pump cycle (p_{high}). This parameter is an important thermodynamic parameter, and it has to be optimized in a real system in order to achieve maximum COP, as is obvious by Figure 4. The proper selection of this parameter is able to lead to maximization of the COP and consequently to the minimization of the electricity production. The parametric investigation in Figure 4 shows that the maximum COP is found for 86.47 bar, and it leads to a COP of 4.189, with the electricity consumption to be 2.387 kW. It has to be commented that the optimum high-pressure level is close to the default value of 85 bar which leads to a COP of 4.175, something that indicates that the parametric analysis of this section is conducted for a reasonable selection about the high-pressure level. Moreover, it has to be said that the heat input in the evaporator has a reducing rate with the increase of the pressure level. The next step is the investigation of extra parameters, as they are presented in Figure 5. More specifically, this figure indicates that the increase of the high pressure leads to higher evaporator temperature and higher values of the geothermal fluid in the inlet and the outlet of the evaporator. On the other hand, the overall resistance of the geothermal field per length has a small reducing trend with the increase of the high-pressure level.

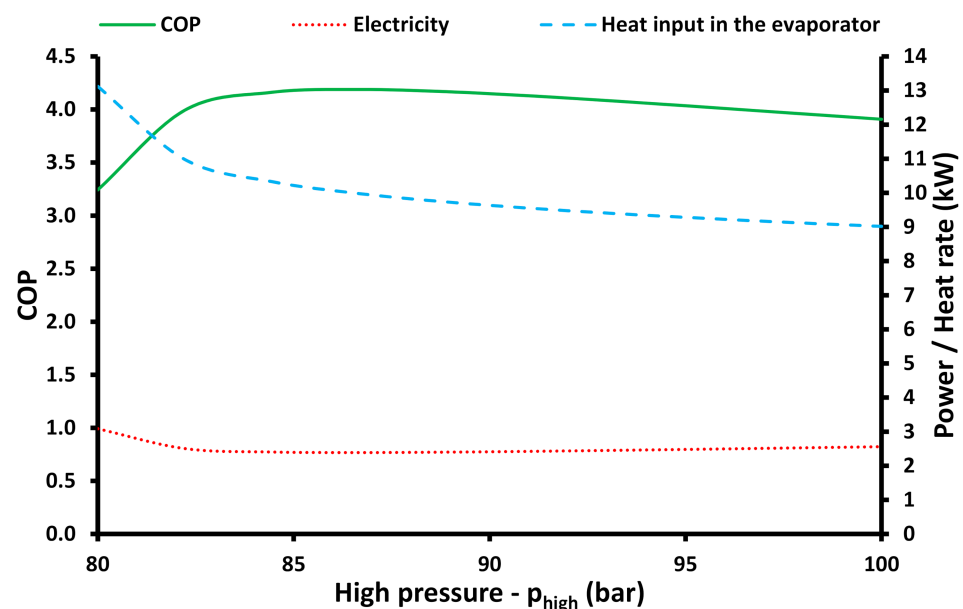


Figure 4. The impact of the high pressure on the COP, electricity consumption and heat input in the evaporator.

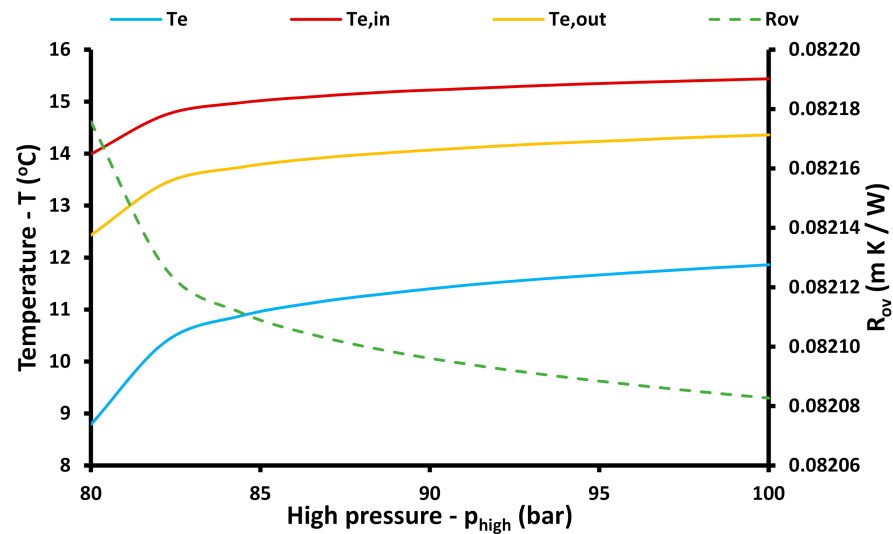


Figure 5. The impact of the high pressure on the evaporator temperature levels and on the overall resistance.

The next examined parameter is the heat exchanger effectiveness (η_{HEX}), and the respective results are illustrated in Figures 6 and 7. It is obvious from Figure 6 that the increase of the heat exchanger effectiveness has a positive effect on the system COP which increases from 4.042 to 4.186. On the other hand, both the electricity consumption and the heat input by the geothermal field have decreasing trends with the increase of effectiveness. Practically, a heat exchanger of higher quality makes better heat recovery inside the cycle, and therefore there is a need for extracting lower quantities of heat from the geothermal field, something that leads to higher evaporator temperature and therefore to higher COP. This result is obvious in Figure 7 which indicates that the evaporator temperature level, as well as the geothermal fluids temperature levels in its inlet and outlet, increases the rate with the increase of the heat exchanger effectiveness. On the other hand, the overall resistance presents a decreasing trend with the effectiveness enhancement. This decrease is not high, and it is reasonable because this variation is only included by the operating temperature levels of the geothermal fluid.

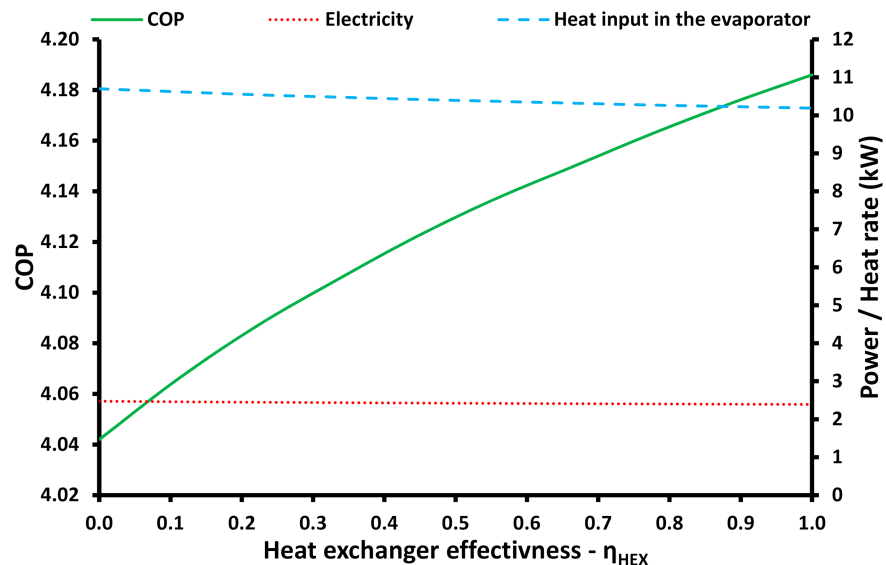


Figure 6. The impact of the heat exchanger effectiveness on the COP, electricity consumption and heat input in the evaporator.

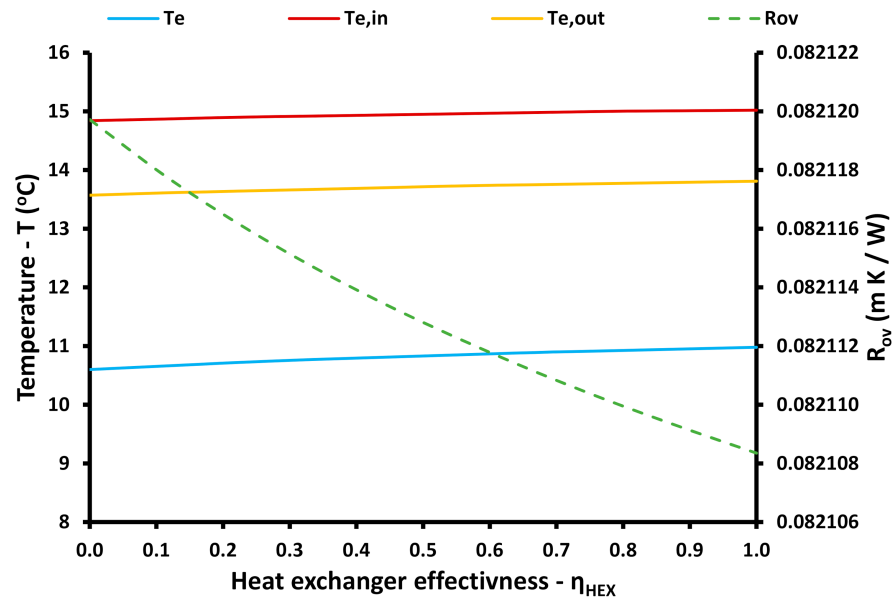


Figure 7. The impact of the heat exchanger effectiveness on the evaporator temperature levels and on the overall resistance.

The next step is the investigation of the CO₂ exit temperature from the heater (T_4) parameter, and the respective results are illustrated in Figures 8 and 9. The increase of this parameter makes the evaporator heat input increase a lot, something that leads also to an electricity consumption increase. The result is the decrease in the COP because the heat production has to be produced in higher temperatures, and this is a more difficult task for the heat pump compared to the cases with small (T_4) levels. Therefore, Figure 8 indicates that the COP is decreased from 4.742 to 3.019 which is a significant result. The conclusion from this result is that the external system that absorbs heat from the heater has to be designed properly in order to operate in the lowest possible temperature levels in order to have high COP. Figure 9 shows that the evaporator temperature levels and the respective geothermal fluids temperatures reduce with the increase of (T_4), while the overall resistance presents a small increase.

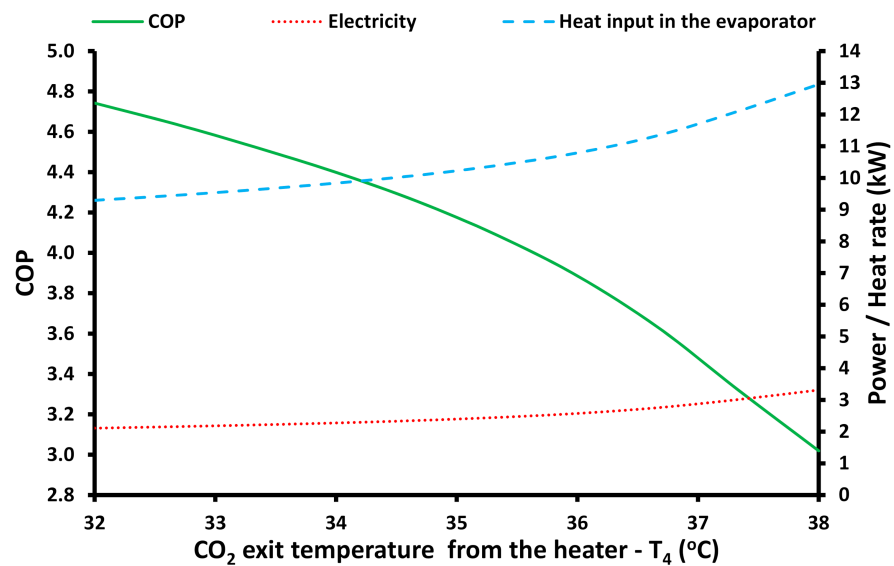


Figure 8. The impact of the CO₂ exit temperature from the heater on the COP, electricity consumption and heat input in the evaporator.

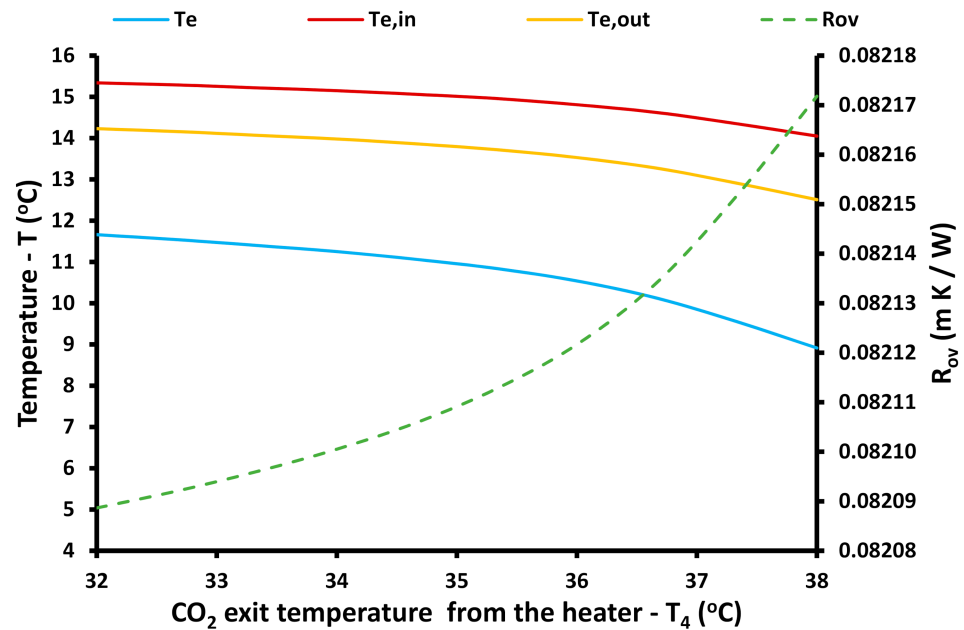


Figure 9. The impact of the CO₂ exit temperature from the heater on the evaporator temperature levels and on the overall resistance.

The next examined parameter is the volumetric flow rate of the geothermal fluid in the evaporator (V_f), and the respective results are exhibited in Figures 10 and 11. This parameter has a small effect on the system performance, and specifically, its increase leads to a rough increase in the COP from 4.155 to 4.186, according to Figure 10. Moreover, the evaporator heat input has a small enhancement with the volumetric flow increase, while the electricity has a small decreasing trend. Figure 11 shows that a higher flow rate increases a bit the evaporator temperature and reduces the temperature difference of the geothermal fluid between the inlet and the outlet of the evaporator. Moreover, the overall resistance has a small decreasing trend with the flow rate enhancement.

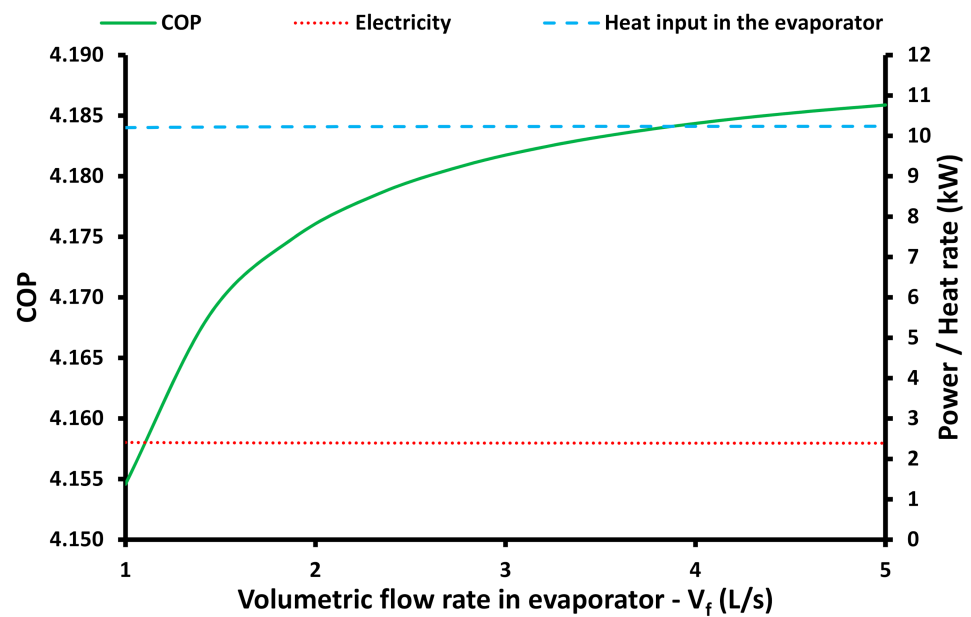


Figure 10. The impact of the volumetric flow rate in the evaporator on the COP, electricity consumption and heat input in the evaporator.

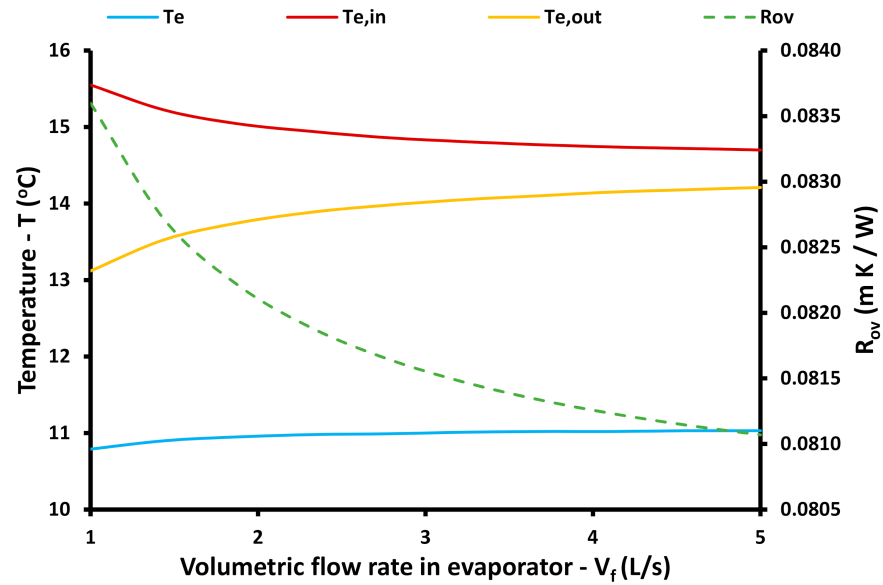


Figure 11. The impact of the volumetric flow rate in the evaporator on the evaporator temperature levels and on the overall resistance.

The last examined parameter in this section is the total thermal transmittance in the evaporator $(UA)_e$, and the respective results are illustrated in Figures 12 and 13. This parameter is an important parameter of the evaporator, and it practically is the responsible device for coupling the two examined subsystems, the heat pump and the geothermal field. The increase of this parameter leads to the increase of the COP, according to Figure 12 because the evaporator temperature also increases according to Figure 13. The COP increases from 3.553 to 4.343 which is an important enhancement, and this fact proves the need for designing a proper heat exchanger for coupling the evaporator with the geothermal field. Moreover, it has to be commented that the increase of the $(UA)_e$ leads to higher heat input in the evaporator because the heat exchanger is greater in this device, while the electricity consumption presents a decrease. The geothermal fluid inlet and outlet temperature present a small decrease with the increase of the total thermal transmittance in the evaporator, as well as does the overall resistance in the geothermal field.

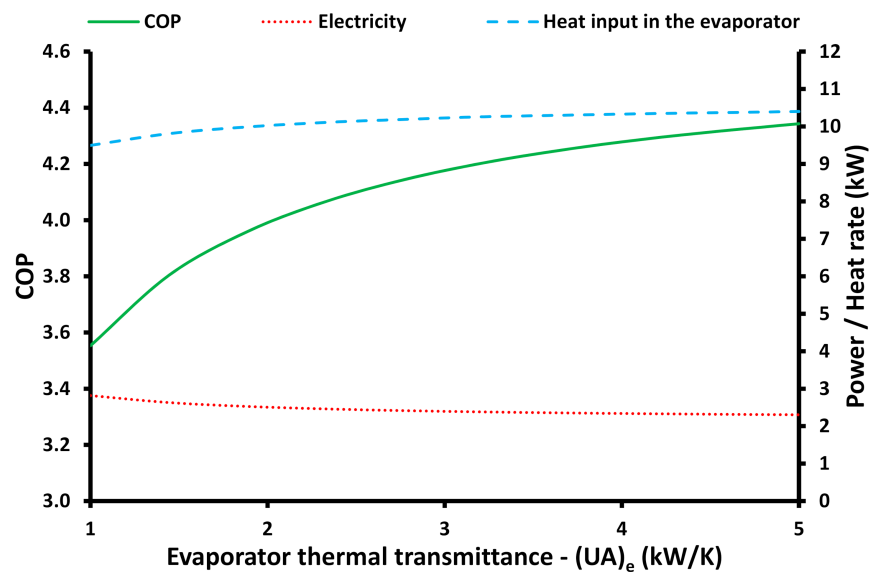


Figure 12. The impact of the evaporator thermal transmittance in the evaporator on the COP, electricity consumption and heat input in the evaporator.

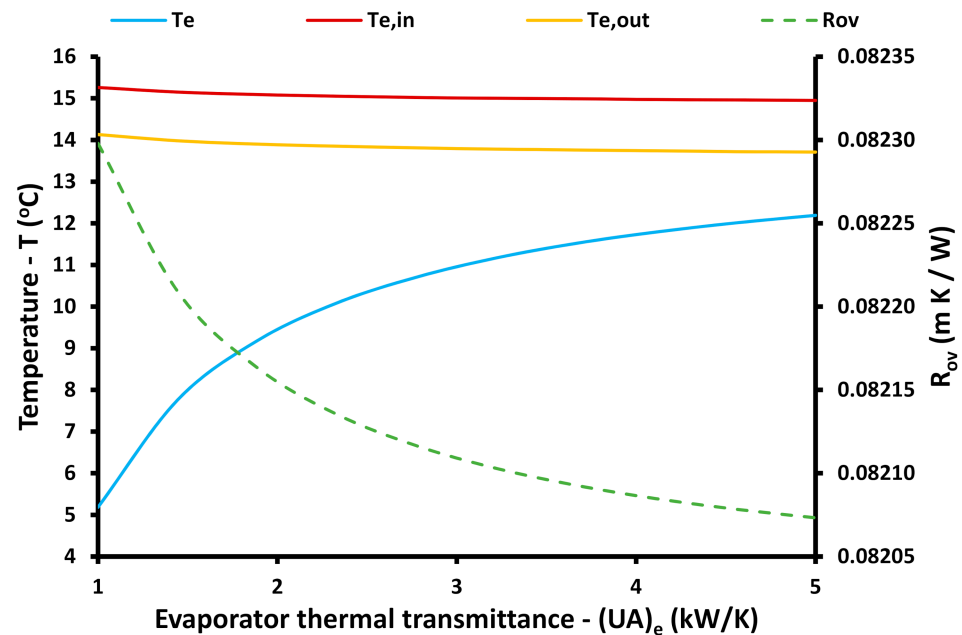


Figure 13. The impact of the evaporator thermal transmittance in the evaporator on the evaporator temperature levels and on the overall resistance.

To sum up, the results of Section 3.2.1 indicate that the COP presents important variation with the variation of the examined parameters and more specifically in the cases that the high pressure, the temperature in the gas cooler exit and the evaporator thermal transmittance are examined. The overall resistance presents rough deviations in this parametric analysis because it is a geothermal field parameter that is only connected with the heat pump through the geothermal fluid temperature levels (inlet and outlet), as well as with its volumetric flow rate. An extra important conclusion from this analysis is the existence of an optimum intermediate high-pressure level, and this fact indicates the need for optimizing this parameter in every design. Lastly, it has to be commented that the less important parameters are the heat exchanger effectiveness and the volumetric flow rate of the geothermal fluid. However, these conclusions are valid for the examined range of the values of the parameters, something that is important to say about the geothermal fluid flow rate because it has to be in the turbulent regime (if it is possible) in order to achieve high heat transfer coefficients in the geothermal field.

3.2.2. Geothermal Field Parameters

The second part of the parametric investigation regards the investigation of parameters that are associated with the geothermal field. More specifically, the studied parameters are the ground mean temperature, the grout thermal conductivity, the inner diameter of the U-tube, the number of the boreholes and the length of every borehole. These parameters can influence the geothermal fluid characteristics, as well as the heat pump performance because they are associated with the selected evaporator temperature and the heat input in the evaporator.

The first examined parameter is the ground mean temperature (T_g), and its investigation is given in Figures 14 and 15. The investigation of different values of these parameters makes possible the simulation of the system in different periods during the year, as well as to different climate zones. The examined range of this parameter is selected to be from 10 °C up to 22 °C in order to cover a great range of possible operating conditions. According to Figure 14, the increase of the ground temperature leads to a significant increase in the COP from 3.372 to 4.620, while the evaporator temperature input also increases and the electricity consumption reduces. Figure 15 shows that the increase of the ground

temperature makes the evaporator temperature, the fluid inlet temperature in the evaporator and the fluid outlet temperature from the evaporator have increasing trends. More specifically, the aforementioned temperature levels increase linearly with the increase of the ground mean temperature which is an interesting result. Lastly, it has to be said also that the overall resistance of the heat exchanger presents a small decrease with the ground source temperature, but this variation has not any effect on the system behavior.

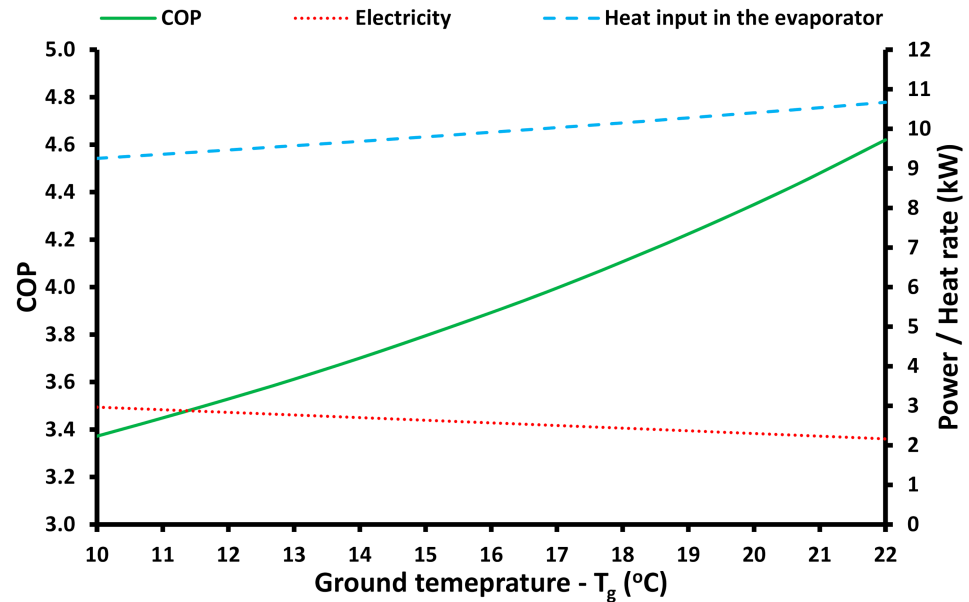


Figure 14. The impact of the ground temperature in the evaporator on the COP, electricity consumption and heat input in the evaporator.

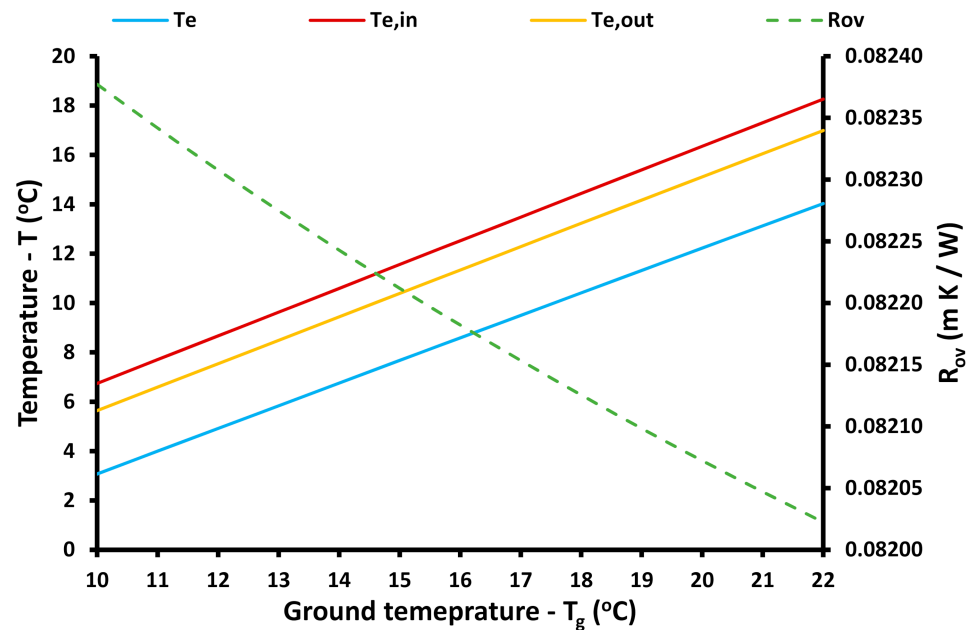


Figure 15. The impact of the ground temperature in the evaporator on the evaporator temperature levels and on the overall resistance.

The next examined parameter is the grout thermal conductivity (k_{grt}) which is dependent on the borehole materials that fill the hole. Figure 16 shows the impact of the grout thermal conductivity on the heat pump performance, and it can be concluded that the higher concavity value leads to a COP improvement from 3.614 to 4.284. In order to

achieve a relatively satisfactory COP, the thermal conductivity has to be at least 1.5 W/mK according to the found results. The evaporator heat inputs increase and the electricity consumption reduces with the increase of the thermal conductivity of the grout material. Figure 17 shows that the evaporator temperature and consequently the geothermal fluid temperatures are getting higher with the increase of the grout conductivity. Moreover, the overall resistance presents a significant decrease with the increase of the thermal conductivity which is an interesting result. More specifically, the increase of the thermal conductivity from 0.5 W/mK to 4 W/mK reduces the thermal resistance per length from 0.199 mK/W to 0.065 mK/W. This result shows that higher thermal conductivity reduces the thermal resistance, and therefore, the heat is transferred easily from the ground to the U-tube.

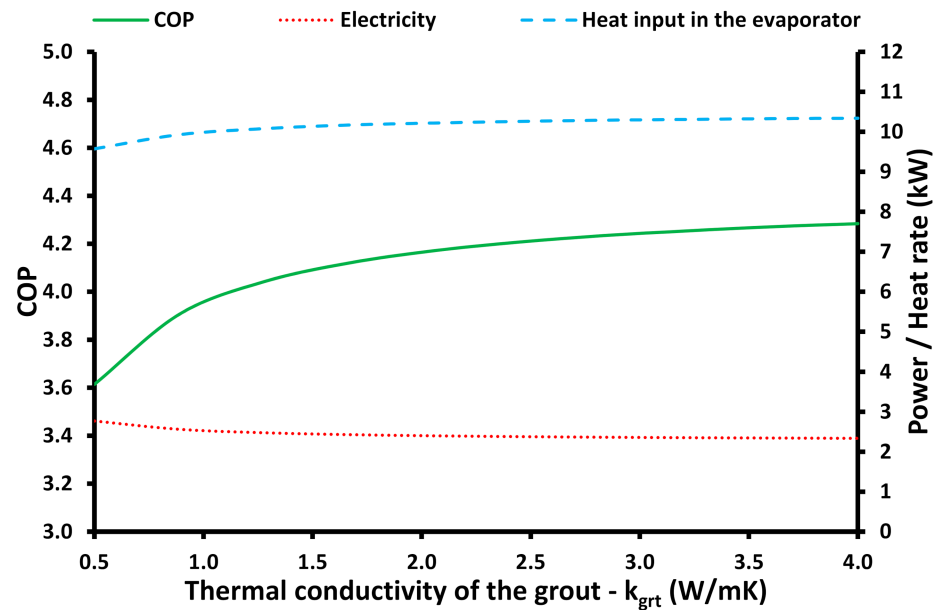


Figure 16. The impact of the grout thermal conductivity on the COP, electricity consumption and heat input in the evaporator.

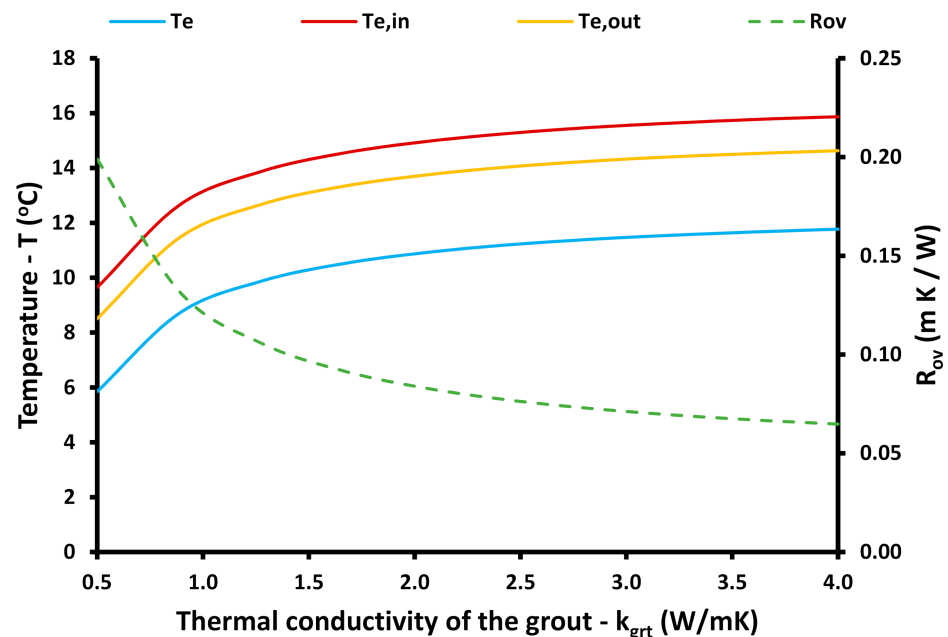


Figure 17. The impact of the grout thermal conductivity on the evaporator temperature levels and on the overall resistance.

The inner diameter of the U-tube (d_{in}) is the next studied parameter, and the results are depicted in Figures 18 and 19. It has to be said that in every case, the thickness of the eth tube is kept constant at 3.5 mm. Figure 18 proves that the use of a tube with a higher diameter leads to an increase in the COP from 4.012 to 4.296 and leads to higher heat input in the evaporator and to lower electricity consumption by the compressor. Figure 19 indicates that the higher diameter of the tube brings the evaporator temperature level and the geothermal fluid temperatures to higher values. However, the overall resistance has a decreasing trend from 0.1111 mK/W to 0.0629 mK/W.

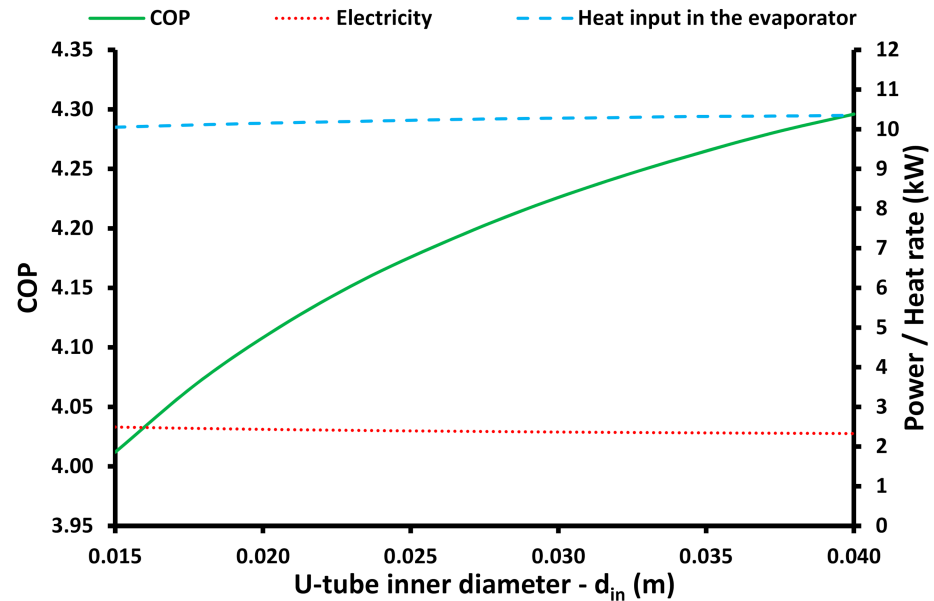


Figure 18. The impact of the U-tube inner diameter on the COP, electricity consumption and heat input in the evaporator.

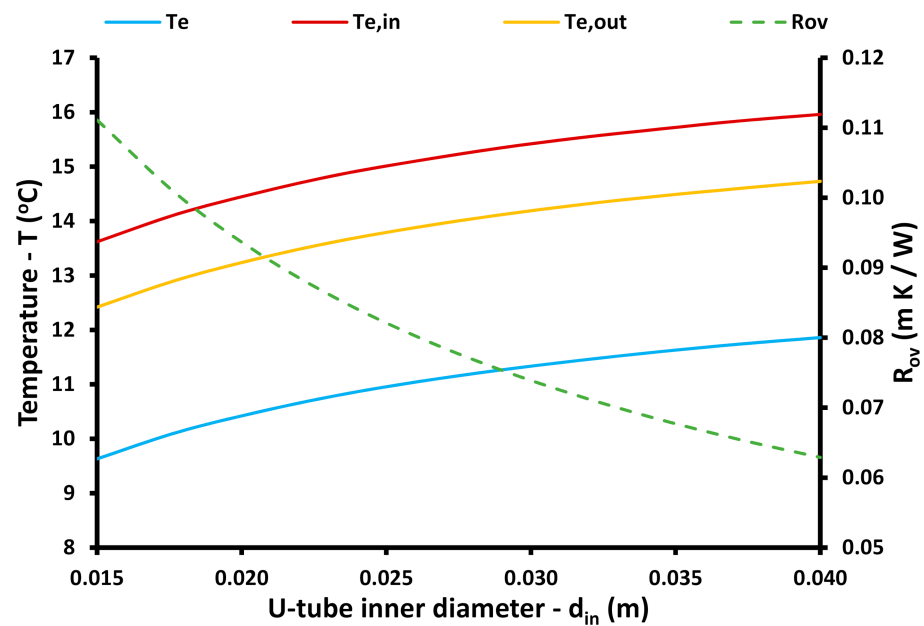


Figure 19. The impact of the U-tube inner diameter on the evaporator temperature levels and on the overall resistance.

The impact of the boreholes number (N) on the system performance is depicted in Figures 20 and 21. It is found that the COP presents a significant increase from 3.211 to

4.501 with the increase of the boreholes from 1 to 10 according to Figure 20. Moreover, the heat input in the evaporator increases while the electricity consumption reduces when there are more boreholes. Figure 21 indicates that the evaporator temperatures and the geothermal fluid temperature levels increase with the higher number of boreholes. Moreover, the thermal resistance has a linearly increasing rate with the increase of the boreholes from 0.081 mK/W to 0.084 mK/W.

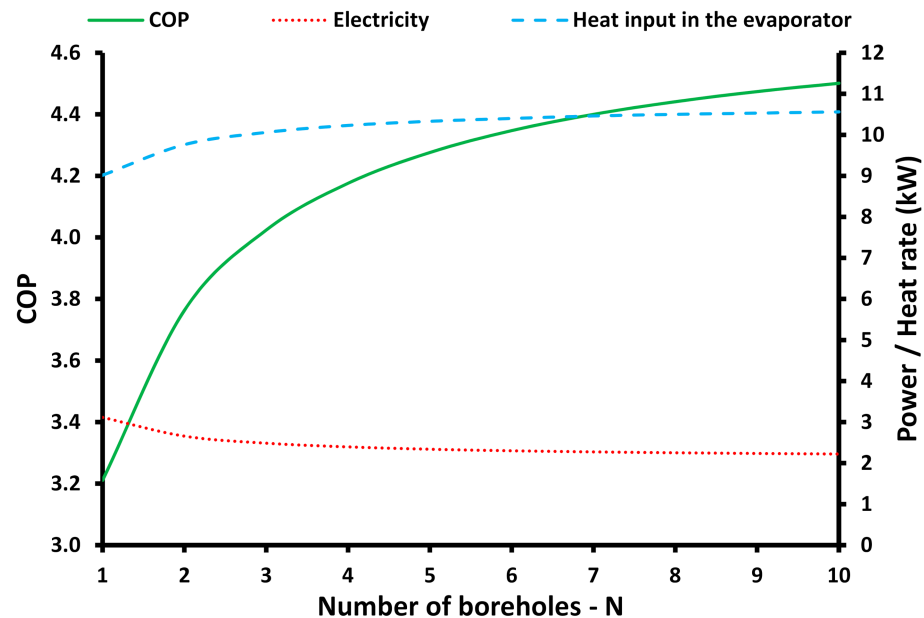


Figure 20. The impact of the number of the boreholes on the COP, electricity consumption and heat input in the evaporator.

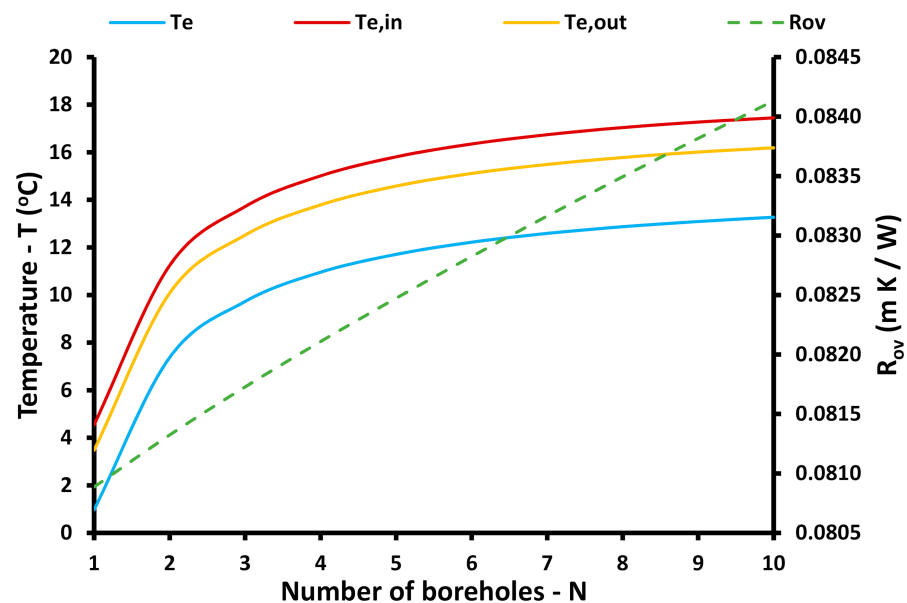


Figure 21. The impact of the number of the boreholes on the evaporator temperature levels and on the overall resistance.

The last examined parameter in the present section is the length of the borehole, (L_{bore}) and the respective results of the parametric analysis are exhibited in Figures 22 and 23. It is found that the COP presents a significant increase from 3.558 to 4.446 with the increase of borehole length according to Figure 22. Furthermore, the heat input in the evaporator increases while the electricity consumption reduces when there are more boreholes. Figure 23

indicates that the evaporator temperatures and the geothermal fluid temperature levels increase with the higher borehole length. Moreover, the thermal resistance has a small decreasing rate with the increase of the boreholes from 0.082288 mK/W to 0.08205 mK/W.

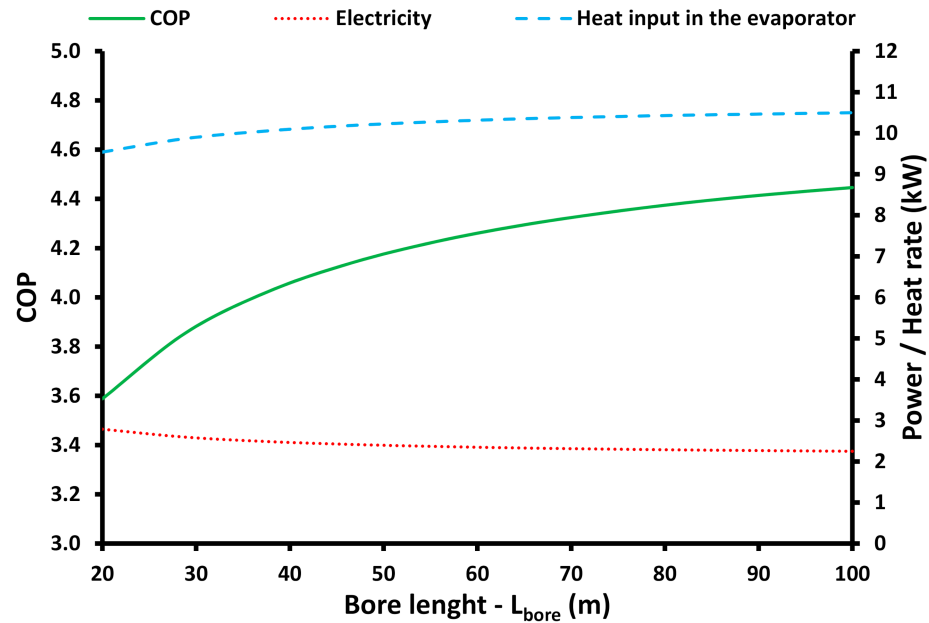


Figure 22. The impact of the borehole length on the COP, electricity consumption and heat input in the evaporator.

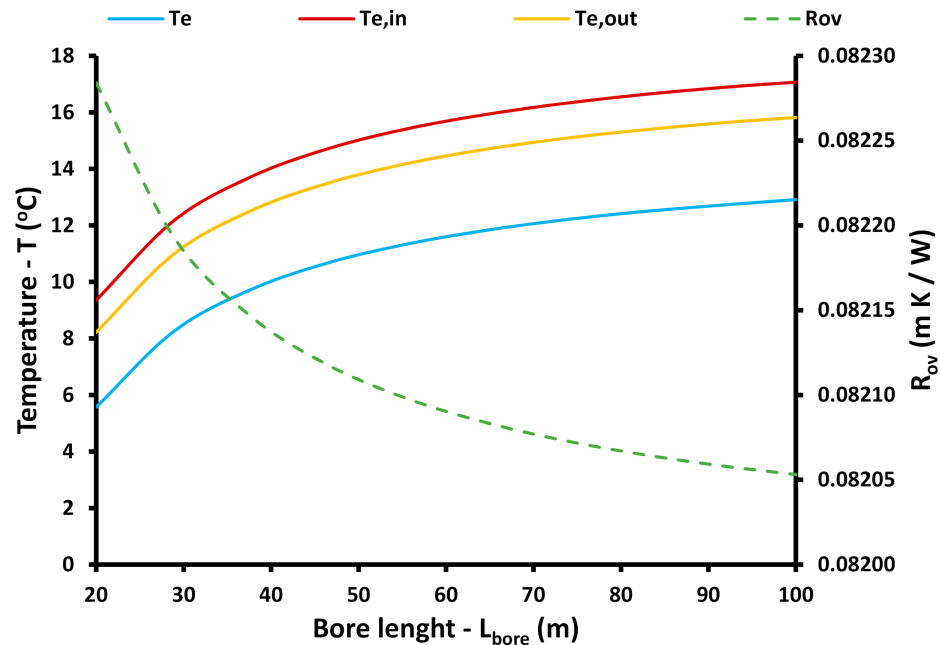


Figure 23. The impact of the borehole length on the evaporator temperature levels and on the overall resistance.

At this point, it is important to summarize the main conclusions from the parametric analysis of the geothermal field. It is found that all the examined parameters have a positive impact on the COP with the ground temperatures and the number of the boreholes being the most effective parameters on the COP. The diameter of the U-tube is the less effective parameter on the system COP. The overall thermal resistance is found to be included by the U-tube diameter and from the grout thermal conductivity in an important way.

3.3. Discussion of the Results

The present work regards a parametric investigation of ten different parameters which regard the heat pump and the geothermal field. The most important parameter for the characterization of the system is the COP, and for this reason, Table 5 summarizes the data about the COP from all the parametric studies. More specifically, Table 5 includes the ten examined parameters, the minimum and maximum examined values of them, and the COP value in these cases. For the case of the high-pressure investigation, there is an internal point that maximizes the COP, and also this point is given. It has to be commented that the results and the conclusions of the present parametric study are valid for the ranges of the examined parameters that are included in Table 1.

Table 5. COP analysis for the various parameters variation.

Parameter	Value	COP	Comment
High pressure (p_{high})	80 bar	3.243	Maximization for an intermediate value
	86.47 bar	4.189	
	100 bar	3.908	
Heat exchanger effectiveness (η_{HEX})	0%	4.042	Monotonically increasing (\nearrow)
	100%	4.186	
Temperature in the heater outlet (T_4)	32 °C	4.742	Monotonically decreasing (\searrow)
	38 °C	3.019	
Volumetric flow rate in the evaporator (V_f)	1 L/s	4.115	Monotonically increasing (\nearrow)
	5 L/s	4.186	
Thermal transmittance in the evaporator (UA_e)	1 kW/K	3.553	Monotonically increasing (\nearrow)
	5 kW/K	4.343	
Ground temperature (T_g)	10 °C	3.372	Monotonically increasing (\nearrow)
	22 °C	4.620	
Thermal conductivity of the grout (k_{grt})	0.5 W/mK	3.614	Monotonically increasing (\nearrow)
	4.0 W/mK	4.284	
Inner diameter of the U-tube (d_{in})	0.015 m	4.012	Monotonically increasing (\nearrow)
	0.040 m	4.296	
Number of boreholes (N)	1	3.211	Monotonically increasing (\nearrow)
	10	4.501	
Bore length (L_{bore})	20 m	3.588	Monotonically increasing (\nearrow)
	100 m	4.446	

According to Table 5, the eight parameters have a positive influence on the COP when they increase, while only the parameter (T_4) increase leads to lower COP. The investigation of the high pressure shows that the COP is maximized for high pressure at 86.47 bar, and in this case, the COP is 4.189. In order to evaluate properly the impact of every parameter on the COP, Figure 24 shows the ratio of the maximum to the minimum COP values that are found during the parametric studies. The parameters are ranked from the less influential to the COP up to the most influential parameters. The less effective parameters on the COP are the volumetric flow rate, the heat exchanger effectiveness and the diameter of the U-tube with $COP_{\text{max}}/COP_{\text{min}}$ ratio at 1.017, 1.036 and 1.071, respectively. The next group includes parameters with a higher influence on the COP. The thermal conductivity of the grout leads to a 1.185 ratio, the thermal transmittance of the evaporator to 1.222, the bore length to 1.239 and the high pressure to 1.292. The most effective parameters on the COP ratio are the ground temperatures with a 1.370 ratio, the number of boreholes with a 1.402 ratio and the temperatures in the heater outlet with a 1.571 ratio. Therefore, this ranking evaluation makes clear which parameters have to be taken into account in any design, optimization and evaluation procedure in order to study properly the system.

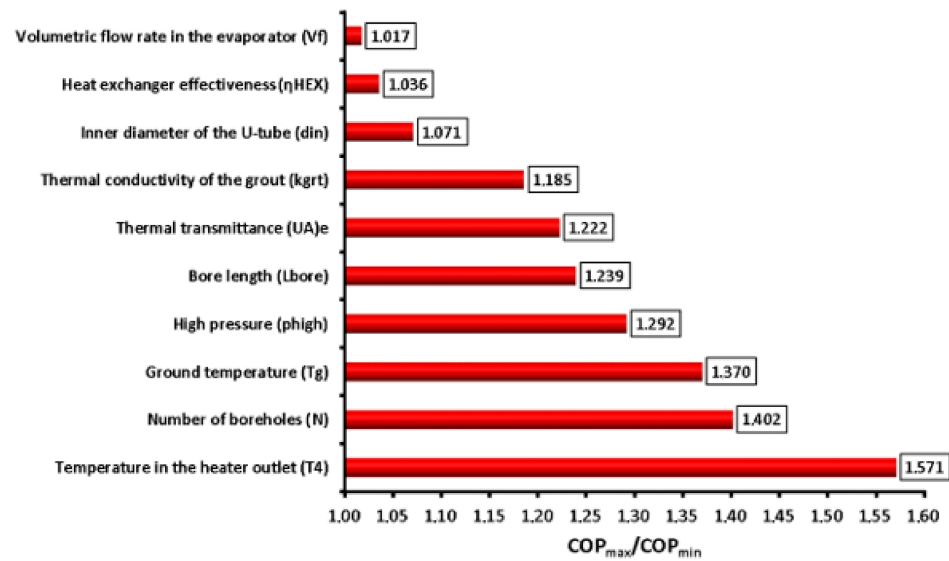


Figure 24. Ranking of the parameters according to the influence on the COP in the examined range.

The next factor that has to be commented on regards the overall resistance of the geothermal heat exchanger per length (R_{ov}). This parameter presents significant variation only when there is a change in the grout thermal conductivity and in the inner diameter of the U-tube. There is also a variation in its value when there is variation in the boreholes number and in the geothermal fluid flow rate. In the rest of the cases, the deviation in the (R_{ov}) is not significant and not important to comment on it.

In the future, there is a need for investigating this system on a seasonal basis and to conduct parametric studies by taking into consideration the variation of the operating conditions during the winter period. Extra parameters like the variation of the heating load among the months can be also considered. Furthermore, the analysis can include financial evaluation and also a comparison with other geothermal designs (e.g., vertical heat exchangers). Lastly, the use of the geothermal field for the summer period as the heat sink for rejecting heat is another idea that can be considered in future work. Moreover, there is a need to examine the use of a horizontal geothermal field and to compare it energetically and financially with the vertical geothermal field.

4. Conclusions

The objective of the present work is the parametric investigation of a geothermal-driven heat pump with CO_2 as the working fluid in the thermodynamic cycle. The system is studied by investigating ten different parameters, as well as a typical default operating scenario is presented in detail. Five parameters about the heat pump system and five parameters about the geothermal field are selected to be studied parametrically. The goal of this parametric investigation is the determination of the impact of every parameter on the system performance. The results of this work indicate how to select the design parameters in order to achieve high efficiency. Moreover, the mean ground temperature is studied in this work which is an operating parameter that is dependent on the location and the month, so the investigation of this parameter leads to the extraction of results about the performance of the system in different locations and periods. The analysis is conducted with a developed model in Engineering Equation Solver which has been successfully validated by using literature results for the heat pump cycle and for the geothermal system. The most important conclusions of the present investigation are given below:

- In the default scenario, the COP is 4.175, the electricity consumption is 2.395 kW, the heat production 10 kW, the heat input in the evaporator from the geothermal field is 10.23 kW, and the heat rejection to the ambient from the gas cooler is 2.625 kW. Moreover,

it has to be said that the overall resistance per length in the geothermal field is found at 0.08211 mK/W.

- The COP is influenced by all the examined parameters. The most influential parameters are the temperature in the heater outlet, the number of the boreholes and the ground temperature which leads to COP_{max}/COP_{min} ratio of 1.571, 1.402 and 1.370, respectively. Lower impact on the COP makes the high-pressure level, the borehole length, the thermal transmittance and the grout thermal conductivity. Small impacts on the COP have the inner U-tube diameter, the heat exchanger effectiveness and the volumetric flow rate of the geothermal fluid.

- The only parameter that has not monotonically impact on the COP is the high pressure of the heat pump cycle. For the default scenario, the optimum high-pressure level is found at 86.47 bar which leads to a COP of 4.189. Therefore, the optimization of the high-pressure level in the transcritical CO₂ heating cycle is an important step in the design of every system.

- The overall geothermal field thermal resistance is more influenced by the grout thermal conductivity and the U-tube inner diameter, while the number of the boreholes and the geothermal fluid volumetric flow rate has a smaller impact on this parameter. The rest of the parameters practically have not an important influence on the overall thermal resistance.

Author Contributions: E.B.: investigation, software, writing and reviewing the original paper; C.T.: supervisions, writing and reviewing the original paper. All authors have read and agreed to the published version of the manuscript.

Funding: This research received no external funding.

Institutional Review Board Statement: Not applicable.

Informed Consent Statement: Not applicable.

Data Availability Statement: Data available after request.

Conflicts of Interest: The authors declare no conflict of interest.

Nomenclature

b_0	Zero-order parameter of Equation (22)
b_1	First-order parameter of Equation (22)
$c_{p,f}$	Geothermal fluid specific heat capacity, kJ/kgK
d_{in}	U-tube inner diameter, m
d_{out}	U-tube outer diameter, m
d_p	Borehole diameter, m
h	Specific enthalpy of the CO ₂ , kJ/kg
h_f	Heat convection coefficient between geothermal fluid and U-tube, W/m ² K
k	Thermal conductivity, W/mK
L_{bore}	Borehole length, m
\dot{m}_f	Mass flow rate of all the geothermal fluid, kg/s
$\dot{m}_{f,0}$	Mass flow rate of the geothermal fluid in one borehole, kg/s
\dot{m}_r	Refrigerant (CO ₂) mass flow rate, kg/s
N	Number of the boreholes
Nu	Nusselt number
P_{el}	Electricity consumption in the compressor, kW
Pr_f	Geothermal fluid Prandtl number
p	Pressure, bar
p_{low}	Low pressure in the heat pump, bar
p_{high}	High pressure in the heat pump, bar

Q_e	Heat input in the evaporator from the geothermal field, kW
Q_{heat}	Heating production, kW
Q_{out}	Heat rejection from the gas cooler to the ambient, kW
R_{film}	Fluid film thermal resistance per length, mK/W
R_{grt}	Grout thermal resistance per length, mK/W
R_{ov}	Overall thermal resistance per length, mK/W
R_p	Thermal resistance of the heat exchanger per length, mK/W
R_{tube}	Thermal resistance of the tube per length, mK/W
Re	Reynolds number
s	Specific entropy of the CO ₂ , kJ/kg
T	Temperature, °C
T_g	Ground temperature, °C
$(UA)_e$	Total thermal transmittance of the evaporator, W/K
V_f	Geothermal fluid volumetric flow rate, L/s
<i>Greek Symbols</i>	
ΔT_{lm}	Mean logarithmic difference, K
η_{comp}	Compressor global efficiency
η_{HEX}	Heat exchanger effectiveness
μ_f	Fluid dynamic viscosity, Pa s
ρ_f	Density, kg/m ³
<i>Subscripts and Superscripts</i>	
e	Evaporator
e,in	Evaporator inlet
e,out	Evaporator outlet
f	Geothermal fluid
f,m	Mean geothermal fluid
max	Maximum
min	Minimum
grt	Grout
<i>Abbreviations</i>	
COP	Coefficient of Performance

References

- Garavaso, P.; Bignucolo, F.; Vivian, J.; Alessio, G.; de Carli, M. Optimal Planning and Operation of a Residential Energy Community under Shared Electricity Incentives. *Energies* **2021**, *14*, 2045. [\[CrossRef\]](#)
- Dallapiccola, M.; Barchi, G.; Adami, J.; Moser, D. The Role of Flexibility in Photovoltaic and Battery Optimal Sizing towards a Decarbonized Residential Sector. *Energies* **2021**, *14*, 2326. [\[CrossRef\]](#)
- Fatima, S.; Püvi, V.; Arshad, A.; Pourakbari-Kasmaei, M.; Lehtonen, M. Comparison of Economical and Technical Photovoltaic Hosting Capacity Limits in Distribution Networks. *Energies* **2021**, *14*, 2405. [\[CrossRef\]](#)
- Bellos, E.; Tzivanidis, C. Energetic and financial sustainability of solar assisted heat pump heating systems in Europe. *Sustain. Cities Soc.* **2017**, *33*, 70–84. [\[CrossRef\]](#)
- Bellos, E.; Tzivanidis, C. Performance analysis and optimization of an absorption chiller driven by nanofluid based solar flat plate collector. *J. Clean. Prod.* **2018**, *174*, 256–272. [\[CrossRef\]](#)
- Lebbihiat, N.; Atia, A.; Arıcı, M.; Meneceur, N. Geothermal energy use in Algeria: A review on the current status compared to the worldwide, utilization opportunities and countermeasures. *J. Clean. Prod.* **2021**, *302*, 126950. [\[CrossRef\]](#)
- Chu, Z.; Dong, K.; Gao, P.; Wang, Y.; Sun, Q. Mine-oriented low-enthalpy geothermal exploitation: A review from spatio-temporal perspective. *Energy Convers. Manag.* **2021**, *237*, 114123. [\[CrossRef\]](#)
- Sanner, B.; Karytsas, C.; Mendrinou, D.; Rybach, L. Current status of ground source heat pumps and underground thermal energy storage in Europe. *Geothermics* **2003**, *32*, 579–588. [\[CrossRef\]](#)
- Karytsas, C. Current state of the art of geothermal heat pumps as applied to buildings. *Adv. Build. Energy Res.* **2012**, *6*, 119–140. [\[CrossRef\]](#)
- Michopoulos, A.; Zachariadis, T.; Kyriakis, N. Operation characteristics and experience of a ground source heat pump system with a vertical ground heat exchanger. *Energy* **2013**, *51*, 349–357. [\[CrossRef\]](#)
- Zhang, Q.; Zhang, X.; Sun, D.; Wang, G. Municipal space heating using a ground source absorption heat pump driven by an urban heating system. *Geothermics* **2019**, *78*, 224–232. [\[CrossRef\]](#)
- Emmi, G.; Zarrella, A.; de Carli, M.; Galgaro, A. An analysis of solar assisted ground source heat pumps in cold climates. *Energy Convers. Manag.* **2015**, *106*, 660–675. [\[CrossRef\]](#)
- Sakellariou, E.I.; Wright, A.J.; Axaopoulos, P.; Oyinlola, M.A. PVT based solar assisted ground source heat pump system: Modelling approach and sensitivity analyses. *Sol. Energy* **2019**, *193*, 37–50. [\[CrossRef\]](#)

14. European Commission. *Regulation (EU) No 517/2014 of the European Parliament and of the Council of 16 April 2014 on Fluorinated Greenhouse Gases and Repealing Regulation (EC) No 842/2006*; European Commission: Brussels, Belgium; Luxembourg, 2014.
15. Bellos, E.; Tzivanidis, C. A Theoretical Comparative Study of CO₂ Cascade Refrigeration Systems. *Appl. Sci.* **2019**, *9*, 790. [[CrossRef](#)]
16. Bellos, E.; Tzivanidis, C. Parametric Analysis of a Polygeneration System with CO₂ Working Fluid. *Appl. Sci.* **2021**, *11*, 3215. [[CrossRef](#)]
17. Kim, W.; Choi, J.; Cho, H. Performance analysis of hybrid solar-geothermal CO₂ heat pump system for residential heating. *Renew. Energy* **2013**, *50*, 596–604. [[CrossRef](#)]
18. Eslami-Nejad, P.; Badache, M.; Bastani, A.; Aidoun, Z. Detailed Theoretical Characterization of a Transcritical CO₂ Direct Expansion Ground Source Heat Pump Water Heater. *Energies* **2018**, *11*, 387. [[CrossRef](#)]
19. Molina-Giraldo, N.; Bayer, P.; Blum, P. Evaluating the influence of thermal dispersion on temperature plumes from geothermal systems using analytical solutions. *Int. J. Therm. Sci.* **2011**, *50*, 1223–1231. [[CrossRef](#)]
20. Piga, B.; Casasso, A.; Pace, F.; Godio, A.; Sethi, R. Thermal Impact Assessment of Groundwater Heat Pumps (GWHPs): Rigorous vs. Simplified Models. *Energies* **2017**, *10*, 1385. [[CrossRef](#)]
21. Antelmi, M.; Alberti, L.; Barbieri, S.; Panday, S. Simulation of thermal perturbation in groundwater caused by Borehole Heat Exchangers using an adapted CLN package of MODFLOW-USG. *J. Hydrol.* **2021**, *596*, 126106. [[CrossRef](#)]
22. Antelmi, M.; Alberti, L.; Angelotti, A.; Curnis, S.; Zille, A.; Colombo, L. Thermal and hydrogeological aquifers characterization by coupling depth-resolved thermal response test with moving line source analysis. *Energy Convers. Manag.* **2020**, *225*, 113400. [[CrossRef](#)]
23. F-Chart Software, Engineering Equation Solver (EES). 2015. Available online: <http://www.fchart.com/ees> (accessed on 1 February 2021).
24. Kavanaugh, S.; Rafferty, K. *Geothermal Heating and Cooling, Design of Ground-Source Heat Pump Systems*; ASHRAE: Atlanta, GA, USA, 2014; ISBN 978-1-936504-85-5.
25. YPEKA. *EK407/B/9.4.2010, TOTEE 20701-3/2010, Climate Data of Greece—KENAK*; YPEKA: Athens, Greece, 2010.
26. Minetto, S.; Cecchinato, L.; Brignoli, R.; Marinetti, S.; Rossetti, A. Water-side reversible CO₂ heat pump for residential application. *Int. J. Refrig.* **2016**, *63*, 237–250. [[CrossRef](#)]
27. Colburn, A.P. A method of correlating forced convection heat-transfer data and a comparison with fluid friction. *Int. J. Heat Mass Transf.* **1964**, *7*, 1359–1384. [[CrossRef](#)]